

# Sway Control of 3-Cars Crane System Using Proposed Fuzzy-PID Controller

Sahin Yildirim  
Erciyes University, Engineering Faculty,  
Mechatronics Engineering  
Kayseri, Turkey  
sahiny@erciyes.edu.tr

Aysegul Gordebil  
Erciyes University, Institute of Science,  
Mechatronics Engineering  
Kayseri, Turkey  
aysegulgordebil@gmail.com

**Abstract** – This paper presents a novel control approach for 3 cars crane systems. Nowadays; some problems for carrying unpredicted loads of crane systems exist. On the other hand; long loads are very important to carry without touch on other materials in factories. In this simulation study, fuzzy based controllers were designed to control vibrations of 3 cars crane system. The simulation results are improved with MATLAB Simulink<sup>®</sup> and show this kind of controllers will be employed in real time such systems.

**Keywords** – crane; control; sway; Fuzzy; PID

## I. INTRODUCTION

A variety of transportation systems are contrived to accommodate different conveyance needs since antiquity. Technological advances make a significant contribution to these systems. Carrying systems began to ameliorate as occupational safety became prominent.

Crane systems are a branch of transportation systems. They are widely utilized in plenty of industrial areas. Different kinds of cranes exist, including gantry cranes, bridge (overhead) cranes, tower (rotary) cranes and boom cranes. Gantry cranes actualize the hauling process in a rectangular prismatic workspace. Gantry cranes have the same workspace with bridge cranes. Burdens are hoisted on the vertical axis and traversed on the horizontal axis. Improvements in crane systems purpose to warrant both fast and safety crane operation. Fast crane operation returns cost reduction. But fast operations cause to the swinging of the payload. Payload oscillation threatens security. There are lots of research on the gantry and bridge cranes to find an optimal point between fast operation and minimum oscillation. [1]

Ramli et al. [1] present a comprehensive review of crane control strategies discussing the latest research works during the years from 2000 to 2016. Sorensen et al. [2] present a

combined feedback and input shaping controller. Miranda-Colorado and Aguilar [3] presents a methodology for designing controllers that attenuate the payload swing angle in two-dimensional overhead crane systems with varying rope length. Lobe et al. [4] deals with a flatness-based control concept for a three-dimensional gantry crane. Giacomelli et al. [5] present the application of an input-output inversion technique for the open-loop control of an overhead crane. Mori and Tagawa [6] propose a vibration controller for overhead cranes considering limited horizontal acceleration. Lu et al. [7] set up a precise model for dual overhead crane system by utilizing the Lagrangian modeling method. Based on that, a nonlinear control strategy is proposed. Zhao and Huang [8] develop a new method to predict the natural frequency of dual planar cranes with different cable lengths. Smoczek [9] presents the fuzzy logic-based robust feedback anti-sway control system which can be applicable either with or without a sensor of sway angle of a payload. Ouyang et al.

[10] propose an energy-shaping-based nonlinear controller for a double pendulum rotary crane system. Shengzeng et al. [11] propose a controller that is extended by a smooth saturated function so that the initial control effort ensures an upper bound when given zero initial conditions, thus leading to a soft trolley start. Smoczek and Szpytko [12] proposed an evolutionary-based algorithm for fuzzy logic-based data-driven predictive model of time between failures and adaptive crane control system design. Maghsoudi et al. [13] propose an improved unity magnitude zero vibration shaper for payload sway reduction of an underactuated 3D overhead crane with hoisting effects. Alghanim et al. [14] proposed a strategy for generating optimal shaped command-profile for the reduction of residual vibrations in rest-to-rest crane maneuvers.

Crane systems are used to carry the burdens in different shapes and weights. Cart number comes into prominence when stowage has a flat shape or a tidy length on horizontal axes. While most of the research articles focus on one cart

crane systems, scholars rarely consider the two and three carts crane systems. But both of two and three carts crane systems are necessitated for vehicles in factory, building, harbour and port transportations. Three cars crane system has much more laden and its oscillation reduction efficacy is better. Thus, 3 cars crane system is the subject of this study.

Proposed three controllers are applied on the 3 cars crane system model. Results of PID, Fuzzy and Fuzzy-PID controllers are compared. Primarily, mathematical model of the 3 cars crane system is derived utilizing Lagrangian Method. Afterwards, transfer function is reckoned on the purpose of linearization of the system model. Block diagrams of both nonlinear and linear system models are installed on MATLAB/Simulink. Finally output signals are received.

Organization of the paper constituted as follows; theory of the 3 cars crane system is given in section 2. Proposed controllers take place in section 3. Section 4 involves simulation results. Conclusions chapter is 5. Section and references occupy in 6. Section.

## II. THEORY OF THE 3 CARS CRANE SYSTEM

2D system model of the 3 cars crane system is depicted in Fig.1. All cars of the crane system carry one distributed mass payload. Carts are driven by forces  $F_1$ ,  $F_2$  and  $F_3$ . For the non-controlled system, these forces are equal. Proposed controllers adjust these forces according to the best result. Replacement of the cars is symbolised with  $x_1$ ,  $x_2$  and  $x_3$ . These values vary only with the action of cars. Replacement of the load depends on both the movement of cars and the oscillation caused by the movement of cars. Sway angle is denoted by  $\Theta_1$ ,  $\Theta_2$  and  $\Theta_3$  for the vibration of each rope. Rope lengths are selected different from each other.  $\Theta_4$  indicates the sway angle of the payload oscillation.

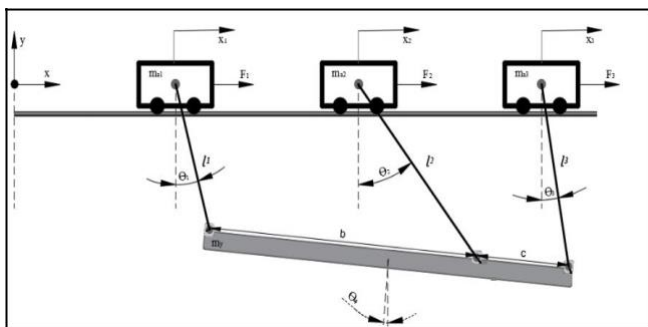


Fig. 1. 2D system model

There are different methods to attain the dynamic equations of a system. Lagrangian Method separates the equation for each element. By taking advantage of this aspect, dynamic equations of forces are attained as follows:

$$F_1 = m_a \ddot{x}_1 + \frac{1}{4} m_y [(1 + l_1)(\ddot{x}_1 + 2\ddot{x}_2 + \ddot{x}_3 + l_1 \ddot{\theta}_1 + 2l_2 \ddot{\theta}_2 + l_3 \ddot{\theta}_3 - (3b + c) \ddot{\theta}_4) + gl_1 \theta_1] \quad (1)$$

$$F_2 = m_a \ddot{x}_2 + \frac{1}{2} m_y [(1 + l_2)(\ddot{x}_1 + 2\ddot{x}_2 + \ddot{x}_3 + l_1 \ddot{\theta}_1 + 2l_2 \ddot{\theta}_2 + l_3 \ddot{\theta}_3 - (3b + c) \ddot{\theta}_4) + gl_2 \theta_2] \quad (2)$$

$$F_3 = m_a \ddot{x}_3 + \frac{1}{4} m_y [(1 + l_3)(\ddot{x}_1 + 2\ddot{x}_2 + \ddot{x}_3 + l_1 \ddot{\theta}_1 + 2l_2 \ddot{\theta}_2 + l_3 \ddot{\theta}_3 - (3b + c) \ddot{\theta}_4) + gl_3 \theta_3] \quad (3)$$

$$0 = -\frac{1}{4} m_y (3b + c) (\ddot{x}_1 + 2\ddot{x}_2 + \ddot{x}_3 + l_1 \ddot{\theta}_1 + 2l_2 \ddot{\theta}_2 + l_3 \ddot{\theta}_3 - (3b + c) \ddot{\theta}_4) \quad (4)$$

Assumptions made to extract these equations are given below:

$\sin =$  and  $\cos = 1$  for the small-angle oscillations.

$(\cdot)^2 = 0$

Equation (1), (2) and (3) are rearranged according to input-output relationship between forces and angles.

Nonlinear system formed on MATLAB Simulink is shown in Fig. 2. The first three blocks compound the nonlinear equation between forces ( $F_1$ ,  $F_2$  and  $F_3$ ) and angles (respectively  $\Theta_1$ ,  $\Theta_2$  and  $\Theta_3$ ). The fourth block gives the  $\Theta_4$  value by taking into account the  $\Theta_1$  and  $\Theta_3$  values and involves trigonometric elements. For the first block, the main input is  $F_1$  and the other three inputs supply the effects caused by  $\Theta_2$ ,  $\Theta_3$  and  $\Theta_4$ . In the same way, the other two blocks involve the effects of the angles in the system except themselves. Each block has two outputs and the first output exposes the angle ( $\Theta_1$ ,  $\Theta_2$ ,  $\Theta_3$  and  $\Theta_4$ ). The second output is the effect of the angle and it connects to one of the inputs of the other blocks.

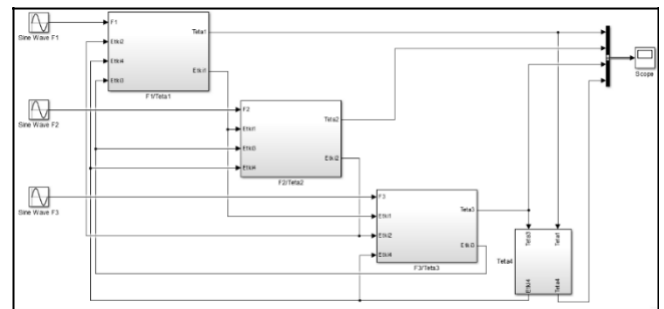


Fig. 2. Block model of nonlinear system

To explain this in detail will be beneficial for the sake of comprehensibility.  $F_1$  manipulates the first cart. But the load, which  $F_1$  affects, is also affected by  $F_2$  and  $F_3$ . Therefore, the first block model, which indicates the relationship between  $F_1$  and  $\Theta_1$ , must also be evaluated for  $F_2$

and  $F_3$ . This consideration is put into practice by using the impressions of the angles, not by using the forces, due to the nonlinear equation.

Fuzzy and Fuzzy-PID controllers entail linear system model, to work accurately. Hence linear system model is obtained using transfer function following invariant system parameters are specified according to the reference crane system. (Rope weight is neglected.)

The transfer function is a main tool for analysing and designing the feedback control system. It describes the system's input-output behaviour [15]. There are two ways to reach the transfer function; state-space matrix and Laplace Transform. In this work, the Laplace Transform is regarded. Laplace Transforms of nonlinear force equations are derived. Afterwards, the transfer matrix method is used as expressed in [16] to acquire the transfer functions of the system.

$$[G(s)] = \begin{bmatrix} G_{11}(s) & G_{12}(s) & G_{13}(s) \\ G_{21}(s) & G_{22}(s) & G_{23}(s) \\ G_{31}(s) & G_{32}(s) & G_{33}(s) \end{bmatrix} \quad (5)$$

$$\begin{bmatrix} \Theta_1 \\ \Theta_2 \\ \Theta_3 \end{bmatrix} = \begin{bmatrix} F_1 \\ F_2 \\ F_3 \end{bmatrix} [G(s)] \quad (6)$$

$$\Theta_1(s) = F_1(s)G_{11}(s) + F_2(s)G_{12}(s) + F_3(s)G_{13}(s) \quad (7)$$

$$\Theta_2(s) = F_1(s)G_{21}(s) + F_2(s)G_{22}(s) + F_3(s)G_{23}(s) \quad (8)$$

$$\Theta_3(s) = F_1(s)G_{31}(s) + F_2(s)G_{32}(s) + F_3(s)G_{33}(s) \quad (9)$$

Transfer matrix is calculated using MATLAB and elements of the Eq. (7), (8) and (9) are drawn from matrix.

Input-output scheme of the noncontrolled system is shown in Figure 3. Main transfer functions are denoted with  $G_i(s)$  ( $i = 1,2,3$ ). Each transfer function has three components, and each component has an input force. Supreme impact for  $\Theta_i$  comes from  $F_i$ . Subordinate effect of  $F_i$  for the other transfer functions is less. But force doesn't change.

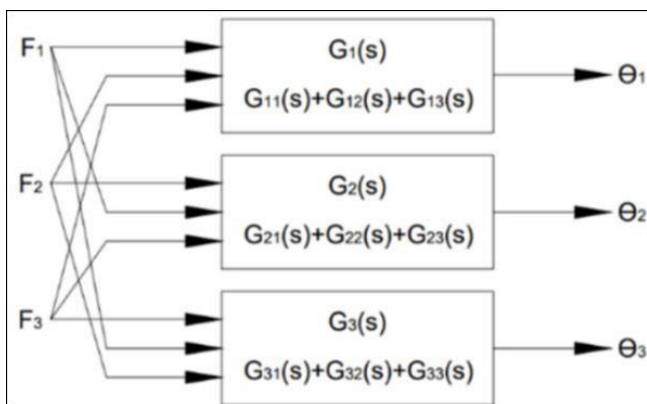


Fig. 3. Input-output scheme of the non-controlled system

For instance;  $F_1$  has the highest effect on  $\Theta_1(s)$ , but it acts on the sway behaviours of  $\Theta_2$  and  $\Theta_3$  less. Thence, all  $F_1$  in the Figure 3 does not change, but the inside structures of the  $G_i(s)$ 's make its influences on the angles different.

According to the scheme in Fig.3, block diagram with STF's is established on MATLAB/Simulink (Fig.4). Moving forces  $F_1$ ,  $F_2$  and  $F_3$  are selected as sinus waves due to the acceleration form of carts. The amplitude of the sinus waves is selected 1 radian for the non-controlled system. In the controlled system, the amplitude is set by the controller. Each angle is achieved via the sum of the outputs of the relevant transfer functions.

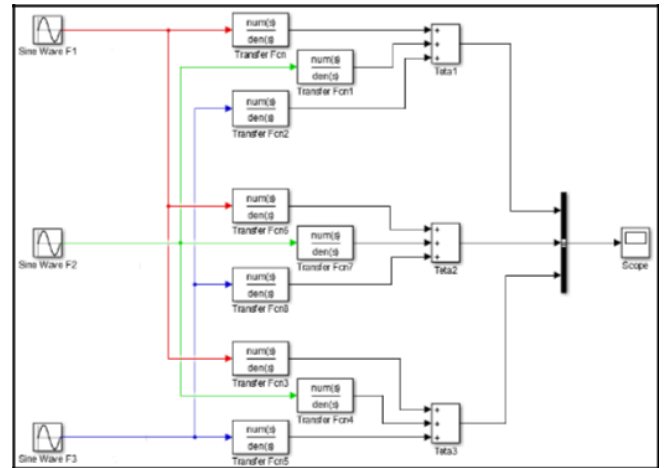


Fig. 4. Block diagram of system with transfer functions

Fig. 5 depicts the input-output relationship in the controlled system. In this instance, inputs are reference signals that express the desired sway angle amplitude and waveform. Even though each reference signal is the same signal, they are pointed out separately for clarity. Outputs are sway angles arose when controllers exert forces. Controllers are denoted with  $C_i(s)$ . Each controller generates the force  $F_i$  to reduce the residual between reference signal  $R_i$  and feedback signal. Feedback signal stems from the output.  $F_i$  has the supreme impact upon the  $\Theta_i$  and it is scattered to the inputs of other STF's without endamaged and switched.  $G_i(s)$  has three components ( $G_{i1}(s)$ ,  $G_{i2}(s)$  and  $G_{i3}(s)$ ) according to the Eq. (7), (8) and (9).

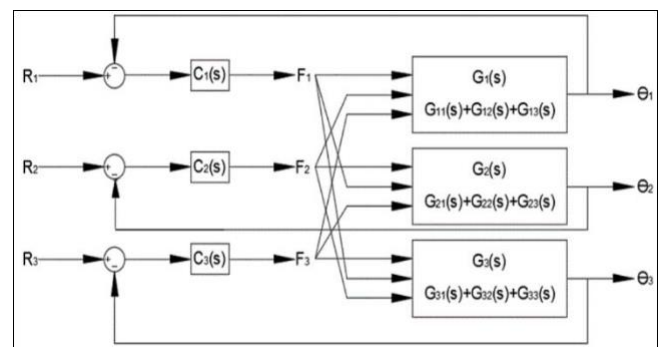


Fig. 5. Input-output scheme of the controlled system

### III. PROPOSED CONTROLLERS

The control aims oscillation reduction for the 3 cars crane system. Oscillation is observed through the angles  $\Theta_1$ ,  $\Theta_2$  and  $\Theta_3$ . The reference angle is a step function and its amplitude stated as 0.001 radian. It accounts for  $0.057^\circ$  degrees. The controller generates the proper force signal which ensures the output to track the reference signal. Three proposed controllers take part in this paper. First, a specimen of using the conventional PID controller is implemented. Second, the Fuzzy controller is deployed on the system. Last, the controlled system is established by fastening the Fuzzy-PID controller. Fuzzy and Fuzzy-PID controllers exploit the same fuzzy rules. PID and Fuzzy-PID controllers adopt different PID techniques. The PID controlled system is installed using Simulink PID module. The PID model handled in the work of Baburajan [17] is integrated in Fuzzy-PID controlled system.

#### A. PID Controller

PID controller is frequently preferred in control applications. The conventional PID controller is a linear controller, which takes the proportion (P), integration (I) and differential (D) of the deviation as the input variables for the control function that will produce the output acting on the target [17].

A proportional controller ( $K_p$ ) will have the effect of reducing the rise time and will reduce but never eliminate the steady-state error. An integral control ( $K_i$ ) will have the effect of eliminating the steady-state error for a constant or step input, but it may make the transient response slower and create oscillations. A derivative control ( $K_d$ ) will have the effect of increasing the stability of the system, reducing the overshoot, and improving the transient response [17].

For the system established in this work,  $K_p$ ,  $K_i$  and  $K_d$  parameters are tuned by MATLAB using autotune option for each system. Then, parameters which give the best result are adjusted as parameters of the other two PIDs.

Block diagram of PID controlled system is depicted in Fig. 6. Model is erected abide by the input-output scheme in Fig. 5.

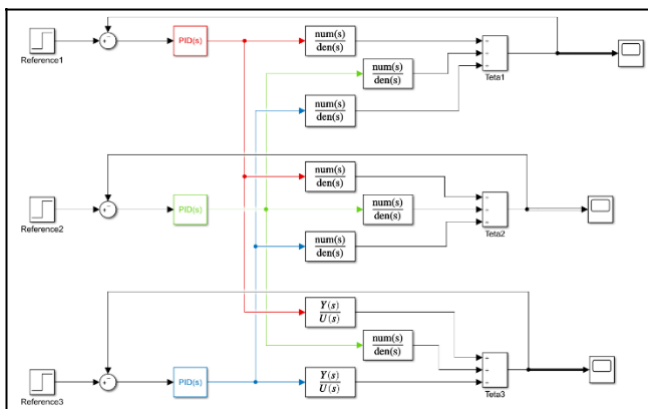


Fig. 6. PID controlled system

Input signals are step function shaped reference angles. The value of the reference sway angle is 0.001 radian. PID controllers try to reduce the gap between the input signal and the feedback signal. PID controllers procure convenient moving forces  $F_{1PID}$ ,  $F_{2PID}$  and  $F_{3PID}$ . Each force operates the three predetermined transfer functions. Outputs are the angles that get by totalling the outputs of the pertinent three transfer functions.

#### B. Fuzzy Controller

Fuzzy control theory is an automatic control theory based on fuzzy set theory, the form of fuzzy language knowledge representing and reasoning, and fuzzy logic rules to simulate the way of thinking and reasoning of human beings [17].

Fuzzy controller is designed considering the fuzzy rules in the thesis of [17]. The variable universe of discourse for the system error  $e$  and the change in error 'ec' is taken as  $[0, 0.01]$ . Then divided it into seven levels, the linguistic values of the 7 fuzzy sets were taken as {NB, NM, NS, Z, PS, PM, PB}, that is {Negative Big, Negative Medium, Negative Small, Zero, Positive Small, Positive Medium, Positive Big} [18].

Membership functions of the fuzzy controller are Gaussian Curve shaped functions. Controller estimates the control parameters depending on the values of error ( $e$ ) and change in error ( $ec$ ). Therefore, there are two inputs of the fuzzy controller. The first input is the error. The second input is taken by differentiating the error. Membership functions of the inputs are depicted in Fig. 7. There are three outputs being  $K_p$ ,  $K_i$ , and  $K_d$ . Each output has the same membership functions with inputs. The variable universe of discourse for the system outputs is taken as  $[0, 1]$  (Fig. 8). Fuzzy rules for  $K_p$ ,  $K_i$ , and  $K_d$  are evinced respectively in Table 1, 2 and 3. Rule surfaces are demonstrated in Fig. 9.

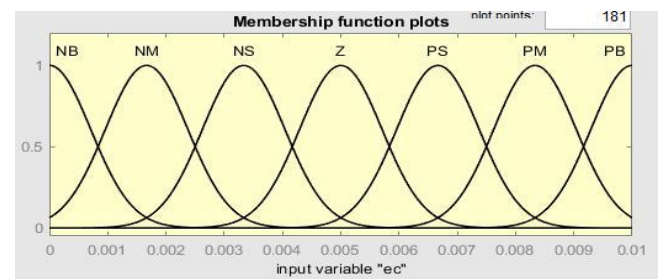


Fig. 7. Membership function plots for inputs

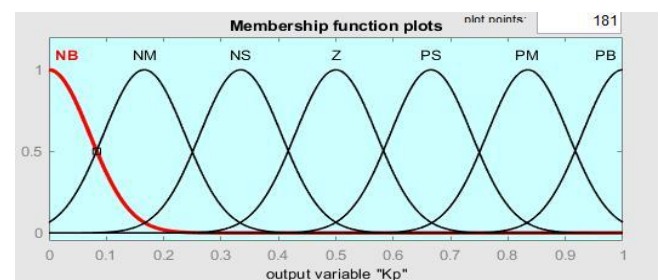


Fig. 8. Membership function plots for outputs

TABLE I. FUZZY RULES OF PROPORTIONAL IMPACT (K<sub>P</sub>)

e	ec						
	NB	NM	NS	Z	PS	PM	PB
NB	PB	PB	PM	PM	PS	Z	Z
NM	PB	PB	PM	PS	PS	Z	NS
NS	PM	PM	PM	PS	Z	NS	NS
Z	PM	PM	PS	Z	NS	NM	NM
PS	PS	PS	Z	NS	NS	NM	NM
PM	PS	Z	NS	NM	NM	NM	NB
PB	Z	Z	NM	NM	NM	NB	NB

TABLE II. FUZZY RULES OF INTEGRAL IMPACT (K<sub>I</sub>)

e	ec						
	NB	NM	NS	Z	PS	PM	PB
NB	NB	NB	NM	NM	NS	Z	Z
NM	NB	NB	NM	NS	NS	Z	Z
NS	NB	NM	NS	NS	Z	PS	PS
Z	NM	NM	NS	Z	PS	PM	PM
PS	NM	NS	Z	PS	PS	PM	PB
PM	Z	Z	PS	PS	PM	PB	PB
PB	Z	Z	PS	PM	PM	PB	PB

TABLE III. FUZZY RULES OF INTEGRAL IMPACT (K<sub>D</sub>)

e	ec						
	NB	NM	NS	Z	PS	PM	PB
NB	PS	NS	NB	NB	NB	NM	PS
NM	PS	NS	NB	NM	NM	NS	Z
NS	Z	NS	NM	NS	NS	NS	Z
Z	Z	NS	NS	NS	NS	NS	Z
PS	Z	Z	Z	Z	Z	Z	Z
PM	PB	NS	PS	PS	PS	PS	PB
PB	PB	PM	PM	PS	PS	PS	PB

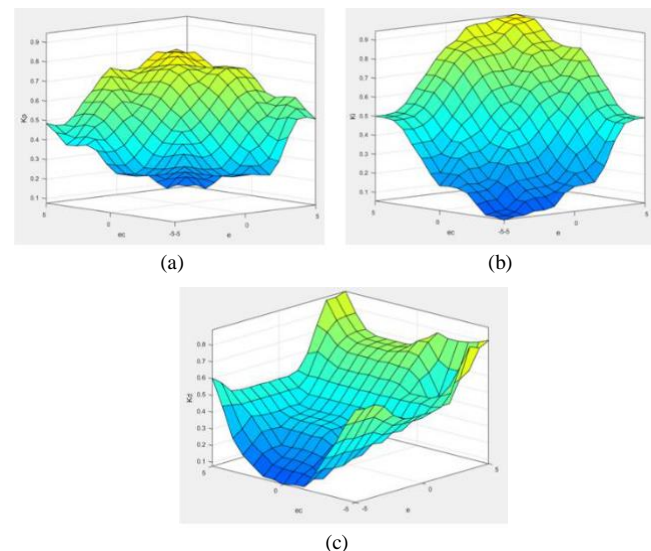


Fig. 9. Rule surfaces; (a) K<sub>p</sub>, (b) K<sub>i</sub>, (c) K<sub>d</sub>

Designed fuzzy controlled system is shown in Fig.10. Input is the desired sway angle. In the Fuzzy controller unit, the memory unit is inserted. The memory unit is obliged due to the loop in the system. Without the memory unit, the Fuzzy

controller doesn't act properly. The second input of the Fuzzy controller is derived by differentiating the error. Derivative element occupies in the subsystem of the Fuzzy controller. Produced forces by the controllers come to the inputs of transfer functions. Angles are attained by the sum of the relevant transfer functions.

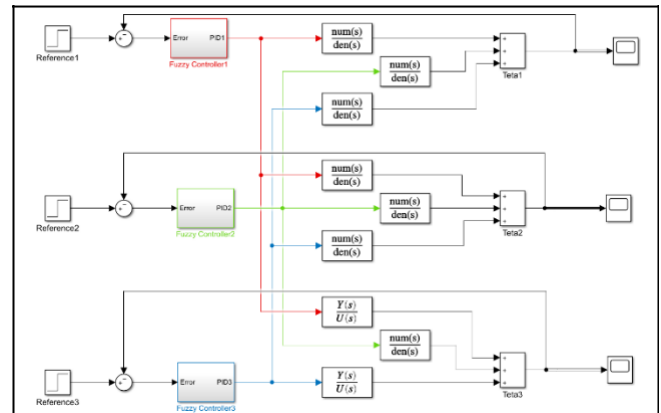


Fig. 10. Fuzzy controlled system

### C. Fuzzy-PID Controller

PID is a traditional technique, considered accurate and simple; its main drawback occurs when applying it to transient system because of the linear characteristic and fixed parameters of controller. Therefore, a self – tuning procedure using fuzzy logic has been implemented to adapt the PID controller parameters according to state of the system [19].

The three parameters of PID controller are to be adjusted based on current deviation and change in deviation as shown below [17].

$$K_p = K_p + \{K_{pfuzzy} * K_p\}$$

$$K_i = K_i + \{K_{ifuzzy} * K_i\}$$

$$K_d = K_d + \{K_{dfuzzy} * K_d\} \tag{10}$$

Proposed Fuzzy PID controlled system is seen in Fig. 11. Inputs are solicited angles which predicate the oscillation limits. The Fuzzy-PID controller computes the optimal force, which causes to the acceptable oscillation, by receiving the disparity between the reference input and the feedback signal. In this case, memory unit is located in the subsystem of controller block. Each force spreads, without diminished or divided, to inputs of wherewithal three transfer functions. Output angles are obtained by the bonding of three relevant transfer functions.

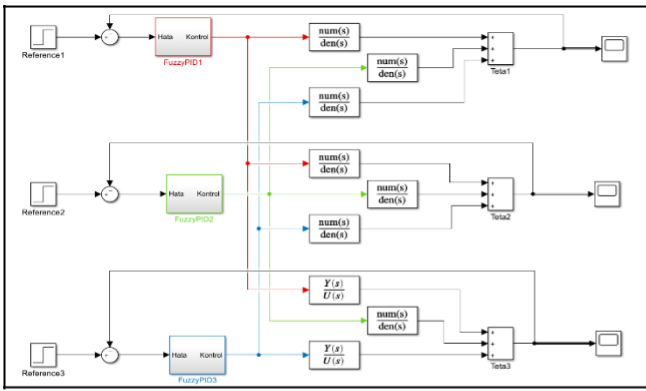


Fig. 11. Fuzzy-PID controlled system

#### IV. SIMULATION RESULTS

Simulations essayed in MATLAB Simulink show the oscillation angle fluctuations clearly. Simulation is activated for 50 seconds. Fig. 12 testifies the oscillations of the three ropes in the non-controlled crane system. The 0.001 radian amplitude reference signal is also placed in graphs.  $\Theta_1$  angle fluctuates in amplitude under  $1.5 \times 10^{-3}$  radian (0.0859 degree).  $\Theta_2$  angle sways maximum  $0.8 \times 10^{-3}$  radian (0.046 degree) and  $\Theta_3$  angle has maximum  $7 \times 10^{-4}$  radian (0.04 degree) oscillation amplitude.

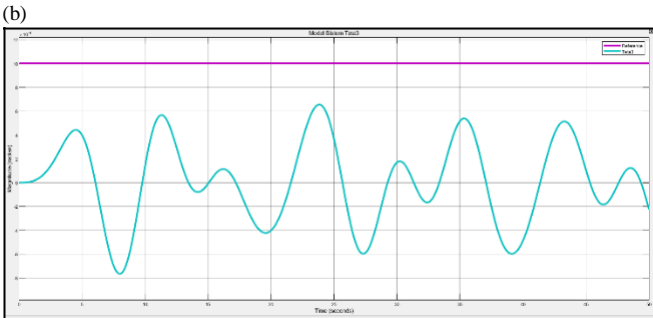
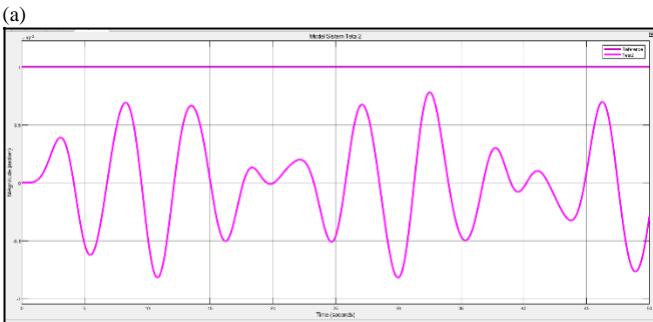
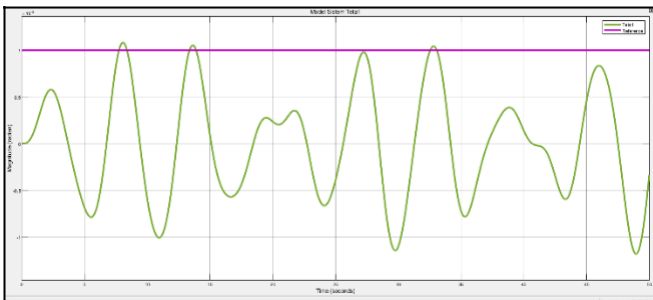


Fig. 12. Outputs of the noncontrolled system, a)  $\Theta_1$ , b)  $\Theta_2$ , c)  $\Theta_3$

Fig. 13. shows the output sway angles  $\Theta_1$ ,  $\Theta_2$  and  $\Theta_3$  of the PID controlled system. It is seen that all three outputs capture the reference signal within the first three seconds. System outputs have a good reference tracking performance under the PID control effect.

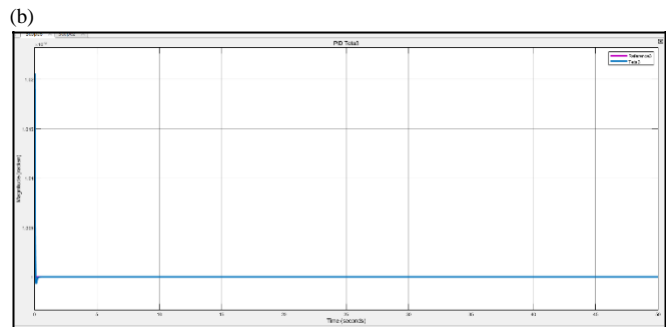
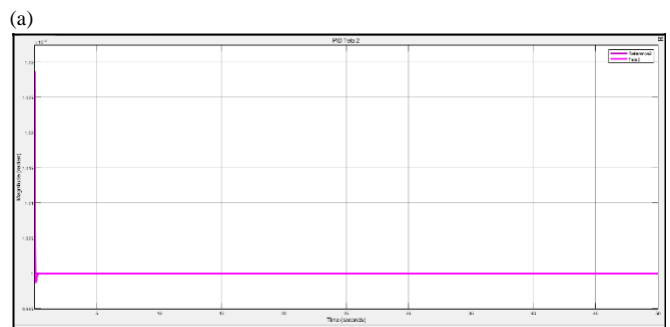
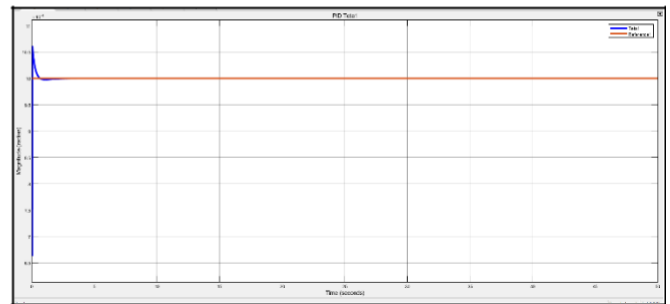
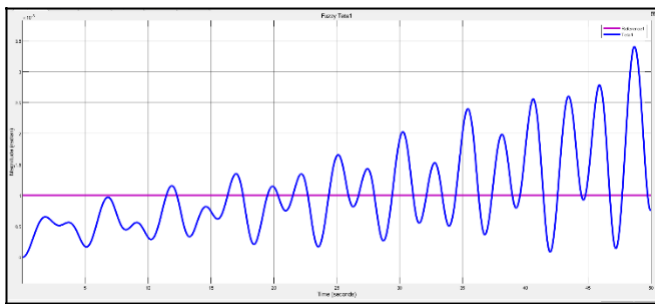
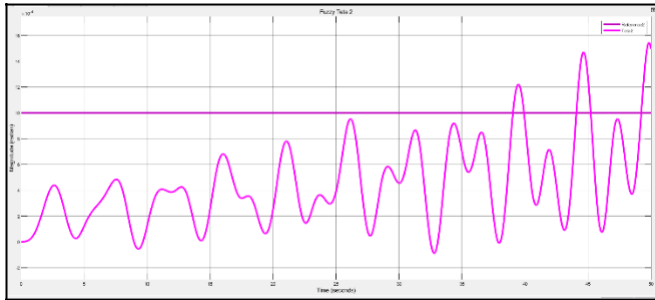


Fig. 13. Outputs of the PID controlled system, a)  $\Theta_1$ , b)  $\Theta_2$ , c)  $\Theta_3$

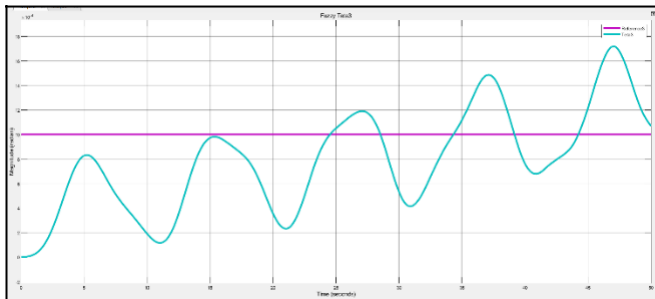
Fig. 14. shows the sway angles  $\Theta_1$ ,  $\Theta_2$  and  $\Theta_3$  of the Fuzzy controlled system. The amplitude of  $\Theta_1$  angle is maximum  $3.4 \times 10^{-3}$  radians (0.195 degrees).  $\Theta_2$  angle has a maximum  $1.55 \times 10^{-3}$  radian (0.088 degrees) amplitude.  $\Theta_3$  angle's sway reaches to  $1.7 \times 10^{-3}$  radian (0.097 degrees) at most. Oscillation under fuzzy control, causes to constitute an untidy wave shape.  $\Theta_3$  angle's wave shape is more consistent than  $\Theta_1$  and  $\Theta_2$ .



(a)



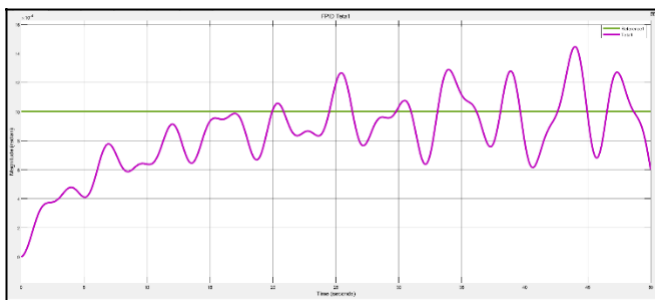
(b)



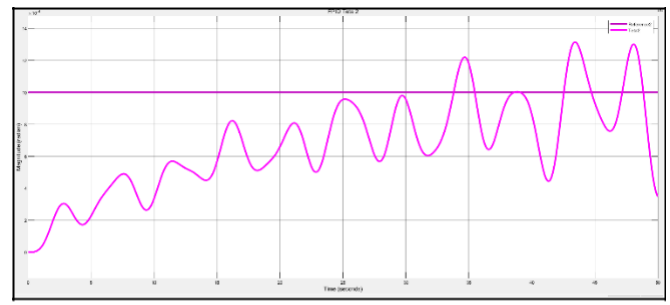
(c)

Fig. 14. Outputs of Fuzzy controlled system, a)  $\Theta_1$ , b)  $\Theta_2$ , c)  $\Theta_3$

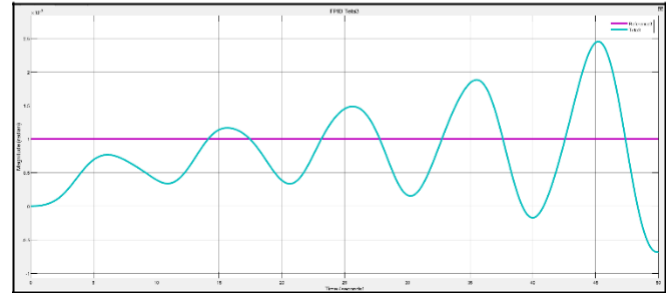
Fig.15 shows the sway angles  $\Theta_1$ ,  $\Theta_2$  and  $\Theta_3$  of the Fuzzy-PID controlled system. The amplitude of  $\Theta_1$  reaches to  $1.45 \times 10^{-3}$  radian (0.083 degree), sway amplitude of  $\Theta_2$  is  $1.5 \times 10^{-3}$  radian (0.086 degree) and  $\Theta_3$  has  $2.45 \times 10^{-3}$  radian (0.14 degree) amplitude. Fuzzy-PID control generates vibration at output angles.  $\Theta_3$  angle's wave shape is more consistent than  $\Theta_1$  and  $\Theta_2$  as occurred in fuzzy control.



(a)



(b)



(c)

Fig. 15. Outputs of Fuzzy-PID controlled system, a)  $\Theta_1$ , b)  $\Theta_2$ , c)  $\Theta_3$

## V. CONCLUSION

This paper has presented a proposed controller approach for 3 cars crane system's pendulum angular variations. The results of fuzzy controller have good performance rather than standard PID controller. This kind of proposed controller structure will be employed in real time applications such systems.

## References

- [1] Ramli, L., Mohamed, Z., Abdullahi, A., M., Jaafar, H., I., Lazim, I., M., 2017, Control strategies for crane systems: A comprehensive review, *Mechanical Systems and Signal Processing*, 95: 1-23
- [2] Sorensen, K., Singhose, W. Dickerson, S., 2005, A controller enabling precise positioning and sway reduction in cranes with on-off actuation, 16th Triennial World Congress, Prague, Czech Republic, Elsevier IFAC Publications, 38(1): 580-585
- [3] Miranda-Colorado, R., Aguilar, L., T., 2019, A family of anti-swing motion controllers for 2D-cranes with load hoisting/lowering, *Mechanical Systems and Signal Processing*, 133: 106253
- [4] Lobe, A., Ettl, A., Steinboeck, A., Kugi, A., 2018, Flatness-based nonlinear control of a three-dimensional gantry crane, *IFAC PapersOnLine*, 22(51): 331-336
- [5] Giacomelli, M., Padula, F., Simoni, L., Visioli, A., 2018, *Mechatronics*, 56: 37-47
- [6] Mori, Y., Tagawa, Y., 2018, Vibration controller for overhead cranes considering limited horizontal acceleration, *Control Engineering Practice*, 81: 256-263
- [7] Lu, B., Fang, Y., Sun, N., 2018, Modeling and nonlinear coordination control for an underactuated dual overhead crane system, *Automatica*, 91: 244-255
- [8] Zhao, X., Huang, J., 2019, Distributed-mass payload dynamics and control of dual cranes undergoing planar motions, *Mechanical Systems and Signal Processing*, 126: 636-648
- [9] Smoczek, J., 2014, Fuzzy crane control with sensorless payload deflection feedback for vibration reduction, *Mechanical Systems and Signal Processing*, 46(1): 70-81

- [10] Ouyang, H., Xu, X., Zhang, G., 2020, Energy-shaping-based nonlinear controller design for rotary cranes with double-pendulum effect considering actuator saturation, *Automation in Construction*, 111: 103054
- [11] Shengzeng, Z., Xiongxiang, H., Haiyue, Z., Qiang, C., Yuanjing, F., 2020, Partially saturated coupled-dissipation control for underactuated overhead cranes, *Mechanical Systems and Signal Processing*, 136: 106449
- [12] Smoczek, J., Szpytko, J., 2014, Evolutionary algorithm-based design of a fuzzy TBF predictive model and TSK fuzzy anti-sway crane control system, *Engineering Applications of Artificial Intelligence*, 28: 190-200
- [13] Maghsoudi, M., J., Ramli, L., Sudin, S., Mohamed, Z., Husain, A., R., Wahid, H., 2019, Improved unity magnitude input shaping scheme for sway control of an underactuated 3D overhead crane with hoisting, *Mechanical Systems and Signal Processing*, 123: 466-482
- [14] Alghanim, K., A., Alhazza, K., A., Masoud, Z., N., 2015, Discrete-time command profile for simultaneous travel and hoist maneuvers of overhead cranes, *Journal of Sound and Vibration*, 345: 47-57
- [15] Piriadarshani, D., Sujitha, S., S., 2018, The role of transfer function in the study of stability analysis of feedback control system with delay, *International Journal of Applied Mathematics*, 31(6): 727-737
- [16] Lobontiu, N., 2017. *System Dynamics for Engineering Students: Concepts and Applications*, Elsevier Science, 786
- [17] Baburajan, S., 2017. *Pitch Control of Wind Turbine Through PID, Fuzzy and Adaptive Fuzzy-PID Controllers*. Rochester Institute of Technology RIT Scholar Works, Master Thesis, Rochester, 62
- [18] Suganthi, L., Iniyan, S., Samuel, A., A., 2015. Applications of fuzzy logic in renewable energy systems – A review, *Renewable and Sustainable Energy Reviews*, 48: 585-607
- [19] Visek, E., Mazzrella, L., Motta, M., 2014. Performance analysis of a solar cooling system using self tuning fuzzy-PID control with TRNSYS. *ISES Solar World Congress*, 2013, Milano, *Energy Procedia*, 57: 2609 – 2618